

RESEARCH

Open Access



Response mechanism of carbon metabolism of *Pinus massoniana* to gradient high temperature and drought stress

Liangliang Li^{1,2}, Yan Li¹ and Guijie Ding^{1*}

Abstract

Background The carbon metabolism pathway is of paramount importance for the growth and development of plants, exerting a pivotal regulatory role in stress responses. The exacerbation of drought impacts on the plant carbon cycle due to global warming necessitates comprehensive investigation into the response mechanisms of Masson Pine (*Pinus massoniana* Lamb.), an exemplary pioneer drought-tolerant tree, thereby establishing a foundation for predicting future forest ecosystem responses to climate change.

Results The seedlings of Masson Pine were utilized as experimental materials in this study, and the transcriptome, metabolome, and photosynthesis were assessed under varying temperatures and drought intensities. The findings demonstrated that the impact of high temperature and drought on the photosynthetic rate and transpiration rate of Masson Pine seedlings was more pronounced compared to individual stressors. The analysis of transcriptome data revealed that the carbon metabolic pathways of Masson Pine seedlings were significantly influenced by high temperature and drought co-stress, with a particular impact on genes involved in starch and sucrose metabolism. The metabolome analysis revealed that only trehalose and Galactose 1-phosphate were specifically associated with the starch and sucrose metabolic pathways. Furthermore, the trehalose metabolic heat map was constructed by integrating metabolome and transcriptome data, revealing a significant increase in trehalose levels across all three comparison groups. Additionally, the *PmTPS1*, *PmTPS5*, and *PmTPPD* genes were identified as key regulatory genes governing trehalose accumulation.

Conclusions The combined effects of high temperature and drought on photosynthetic rate, transpiration rate, transcriptome, and metabolome were more pronounced than those induced by either high temperature or drought alone. Starch and sucrose metabolism emerged as the pivotal carbon metabolic pathways in response to high temperature and drought stress in Masson pine. Trehalose along with *PmTPS1*, *PmTPS5*, and *PmTPPD* genes played crucial roles as metabolites and key regulators within the starch and sucrose metabolism.

Keywords *Pinus massoniana*, High-temperature drought, Carbon metabolism, Trehalose

Background

Carbon metabolism is a crucial metabolic pathway for plant growth and development [1]. The processes encompass photosynthetic carbon assimilation, sucrose and starch metabolism, as well as carbohydrate transport and utilization in plants [2]. Global warming exacerbates the impact of drought on plant carbon cycles. Therefore, comprehensively studying the mechanism of carbon

*Correspondence:

Guijie Ding
gjding@gzu.edu.cn

¹ Forest Resources and Environment Research Center, Key Laboratory of Forest Cultivation in Plateau Mountain of Guizhou Province, College of Forestry, Guizhou University, 550001 Guiyang, China

² Institute of Mountain Resources of Guizhou Province, Guiyang, China 550001



© The Author(s) 2024. **Open Access** This article is licensed under a Creative Commons Attribution 4.0 International License, which permits use, sharing, adaptation, distribution and reproduction in any medium or format, as long as you give appropriate credit to the original author(s) and the source, provide a link to the Creative Commons licence, and indicate if changes were made. The images or other third party material in this article are included in the article's Creative Commons licence, unless indicated otherwise in a credit line to the material. If material is not included in the article's Creative Commons licence and your intended use is not permitted by statutory regulation or exceeds the permitted use, you will need to obtain permission directly from the copyright holder. To view a copy of this licence, visit <http://creativecommons.org/licenses/by/4.0/>. The Creative Commons Public Domain Dedication waiver (<http://creativecommons.org/publicdomain/zero/1.0/>) applies to the data made available in this article, unless otherwise stated in a credit line to the data.

cycling in drought-tolerant plants can enhance predictions regarding dynamic changes in terrestrial carbon budgets in the future [3]. However, the combined effect of high temperature and drought stress on plants surpasses that of individual stresses alone, posing a challenge to investigating plant carbon metabolism under stress conditions [4].

High temperatures and drought stress can lead to a decline in plant photosynthesis and productivity. Sugar, as the product of photosynthetic carbon assimilation, not only provides energy for plants but also plays a crucial role in regulating plant growth and development, metabolic regulation, and stress resistance. Soluble sugars, starch, and other carbohydrate substances in plants act as stage buffers against stress [5]. It has been observed that photosynthesis is more sensitive to high temperatures and drought compared to respiration [6]. To adapt to high-temperature environments, plants increase respiration which results in reduced carbon availability for plant growth [7]. When carbohydrates synthesized through light and carbon fixation fail to meet the catabolic demands under high temperatures and drought conditions, plants redistribute limited carbohydrates within their bodies to enhance utilization efficiency ensuring growth and development under adverse circumstances. This redistribution involves obtaining additional sugars with osmoregulatory properties. However, with increasing severity and duration of high temperature and drought stress, soluble sugar levels significantly decrease within plants [8], ultimately leading to carbon starvation jeopardizing plant survival [9]. Although progress has been made regarding the effects of high temperature and drought on plant carbon metabolism [10], the response mechanism of carbon metabolism towards combined stresses of high temperature and drought remains unclear. Therefore, gaining further insights into core metabolites involved in the carbon metabolism of the drought-resistant pioneer Masson Pine responding to high temperature and drought is crucial for predicting forest ecosystem responses towards climate change.

Masson pine, as a native tree in China and a pioneer representative of drought-resistant plants [11], has been the focus of current studies on carbon metabolism under stress. However, these studies mainly concentrate on photosynthetic carbon fixation or sucrose and starch metabolism [12], without analyzing the comprehensive response mechanism of high temperature and drought throughout the entire cycle of carbon metabolism. It has been observed that drought significantly reduces photosynthesis, stomatal conductance, and soluble sugar content in plants, while high temperature exacerbates this effect by causing a rapid decline in photosynthesis and soluble sugar levels [13]. Moreover, investigations into

sucrose and starch metabolism have revealed that high-temperature treatment can increase the sucrose content in plants [14]. Under conditions of drought or high-temperature drought, both sucrose and starch contents decrease significantly, indicating that drought activates plant's ability to degrade sucrose [15]. The influence of high temperature and drought on plant starch remains controversial. Some studies suggest that certain enzymes involved in starch biosynthesis become inactive at high temperatures, inhibiting the conversion of sucrose into starch which leads to decreased starch content. On the other hand, other research proposes that early cessation of starch accumulation rather than inhibition of enzymes related to its biosynthesis is primarily responsible for reduced starch content at elevated temperatures [16]. Therefore, high temperatures and drought inhibit photosynthetic carbon fixation, sucrose and starch content in plants. In addition, trehalose act as a major osmoprotectant to protect proteins and cell membranes during the dehydration of *Selaginella selaginella* [17] and *Selaginella lepidophylla* [18], resulting in almost complete dehydration of these plants and a return to full viability after rehydration. As a pioneer tree with strong drought tolerance, does trehalose of Masson Pine also play an important role under the cross-stress of high temperature and drought? Therefore, digging into the response mechanism of carbon metabolism of Masson pine to high temperature and drought lays a foundation for understanding the resistance mechanism of pinaceae plants.

Result

Effects of high temperature and drought on photosynthesis in Masson Pine seedlings

The photosynthetic rate of Masson Pine seedlings exhibited similar changes at 25°C, 30°C, and 35°C after being subjected to a 10-day stress period. With increasing drought severity, the photosynthetic rate gradually decreased. Under equivalent levels of drought stress, the photosynthetic rate of Masson Pine seedlings displayed a decreasing trend with rising temperatures. Compared to the control group under non-drought conditions & high temperature (35°C), the photosynthetic rate of Masson Pine seedlings decreased by 37.4%. Similarly, under severe drought at 25°C, the photosynthetic rate of Masson Pine seedlings decreased by 60.3% compared to the control group. When exposed to combined stresses of high temperature and drought (35°C & SD), the photosynthetic rate of Masson Pine seedlings reduced by 83.6% compared to CK at 25°C (Fig. 1A). The changing trend of the photosynthetic rate of Masson Pine seedlings remained consistent with that observed after 10 days, even under a prolonged stress period of 20 days. The photosynthetic rate of Masson Pine seedlings showed

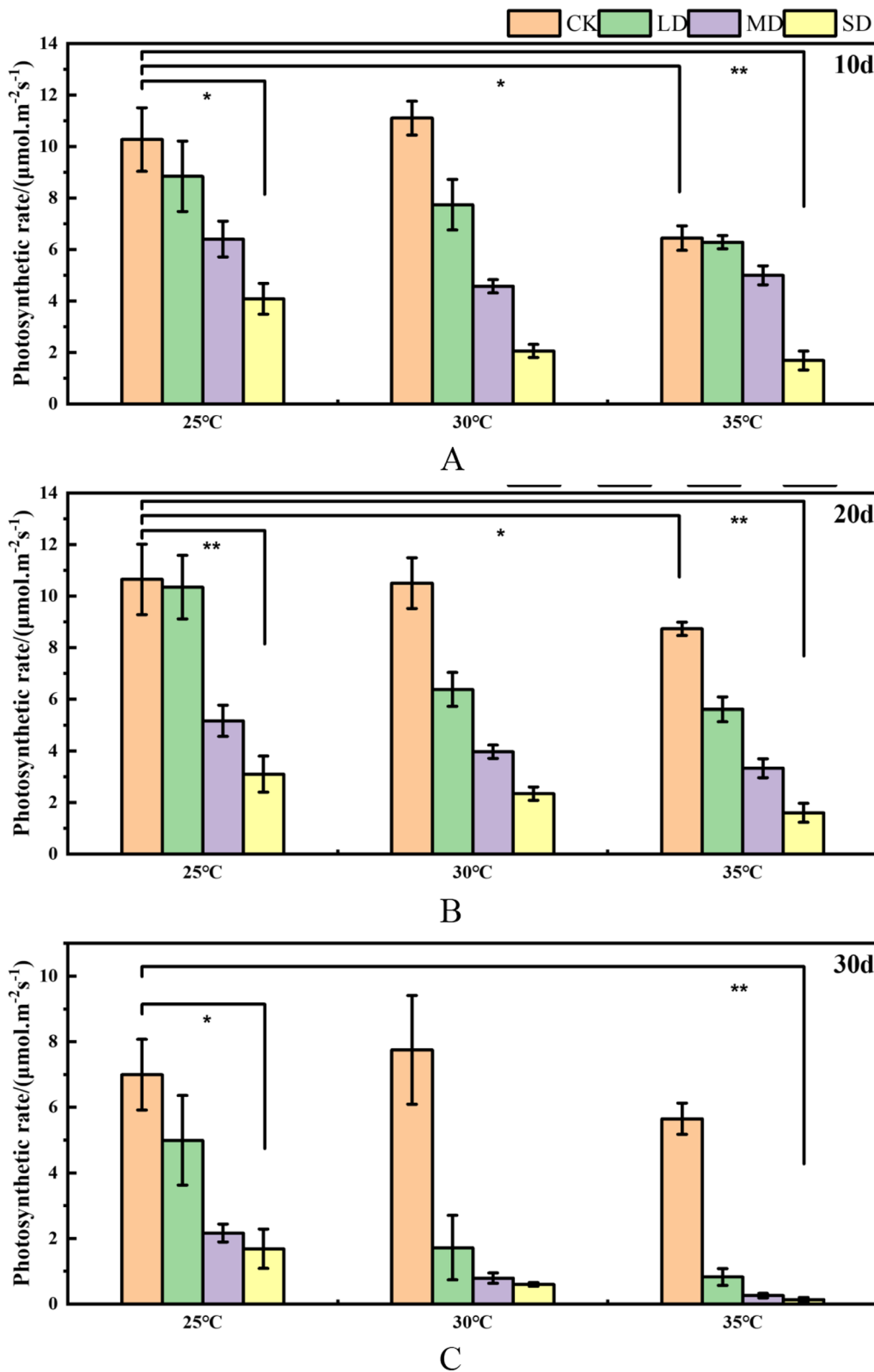


Fig. 1 Effects of high temperature and drought on the photosynthetic rate of Masson pine seedlings. The changes in photosynthetic rate after 10, 20, and 30 days of high temperature and drought stress are represented by Figure. **A, B, C** respectively. (* corresponds to the significance level of 5%, and ** corresponds to the significance level of 1%, CK: 75%-80% FC (field capacity), LD: 55%-60% FC, MD: 40%-45% FC, SD: 30%-35% FC)

similar changes at 25°C, 30°C and 35°C. With the increase of drought, the photosynthetic rate decreased gradually. It was found that the photosynthetic rate of Masson pine seedlings decreased by 18.4% compared with 25°C CK at non-drought and 35°C, while the photosynthetic rate of Masson pine seedlings decreased by 71.0% under severe drought at 25°C compared with 25°C CK. Under the interaction stress of high temperature and drought (35°C & SD), the photosynthetic rate of Masson Pine seedlings decreased by 85.0% compared with 25°C CK (Fig. 1B). Under 30 days of stress, the photosynthetic rate of Masson pine seedlings decreased by 19.2% compared with 25°C CK at no drought and 35°C high temperature, while the photosynthetic rate of Masson pine seedlings decreased by 75.8% under severe drought at 25°C compared with 25°C CK. Under the interaction stress of high temperature and drought (35°C & SD), the photosynthetic rate of Masson Pine seedlings decreased by 98.1% (Fig. 1C).

Effects of high temperature and drought on transpiration of Masson Pine seedlings

The transpiration rate of Masson Pine seedlings exhibited similar changes at 25°C, 30°C, and 35°C after being subjected to a 10-day stress period. As drought intensity increased, there was a gradual decrease in the transpiration rate. The transpiration rate of Masson Pine seedlings exhibited a gradual increase with rising temperatures under equivalent drought conditions. The transpiration rate of Masson's pine seedlings was found to increase by 59.5% compared to the control group (CK) at 25°C under non-drought and 35°C conditions, while it decreased by 84.1% under severe drought at 25°C. Under the interaction stress of high temperature and drought (35°C & SD), the transpiration rate of Masson Pine seedlings decreased by 59.6% compared with CK at 25°C (Fig. 2A). Under the condition of 20 days of stress, the changing trend of the transpiration rate of Masson Pine seedlings was consistent with that of 10 days. The transpiration rates of Masson pine seedlings at 25°C, 30°C, and 35°C exhibited similar patterns, gradually decreasing with increasing drought severity. Compared to CK at both 25°C and 35°C, the transpiration rate of Masson pine seedlings increased by 47.4%, while it decreased by 89.9% under severe drought conditions at only 25 °C. Under the combined stress of high temperature and drought (35 °C & SD), the photosynthetic rate of Masson Pine seedlings decreased by 67.5% (Fig. 2B). Under the condition of stress for 30 days, the transpiration rate of Masson pine seedlings showed a gradual decline with the gradual increase of temperature under control and light drought, while the changing trend was opposite under moderate and severe drought, and the transpiration rate showed a gradual

decline trend, and reached the minimum value under 35°C severe drought (Fig. 2C).

Transcriptome determination of Masson pine under high temperature and drought

The leaves of Masson pine were subjected to different treatments, and their transcriptome data were sequenced using Illumina high-throughput sequencing technology. After sequencing all samples, a comprehensive statistical analysis was conducted on the acquired data, encompassing calculations of Q30 and fuzzy base percentage, as well as percentages for Q20 and Q30 values. The statistical results can be found in Table S1 (Additional File 1). The filtered data can be obtained by utilizing cutadapt to eliminate the 3' end-band joints sequence and discarding reads with an average mass fraction below Q20, as illustrated in Table S2 (Additional File 1). The base mass of each location was determined using the distribution map of single base masses from the sequencing data. Analysis revealed that most sequences had a base mass above 20, indicating high sequencing quality in Fig. S1 (Additional File 1). The further analysis of the distribution of average quality in reads revealed a larger peak value and narrower peak width, indicating an overall high quality. The Fig. S2 presents the results of average quality distribution for selected reads (Additional File 1). The generated raw reads amounted to 46,602,818, out of which 43,923,726 clean reads were obtained after eliminating low-quality reads. The samples exhibited a clean rate of approximately 94.25%, with Q20 and Q30 values reaching 98.22% and 94.68%, respectively (Table 1). These sequencing results are deemed reliable and the data can be utilized for subsequent analysis.

The results were compared against the reference genome

The reference genome index was established using Bowtie2, followed by the comparison of filtered Reads with the Loblolly pine reference genome using Tophat2. The comparison efficiency ranged from 75.69%–76.86% (Table 2), indicating the reliability of the sequencing data for subsequent analysis.

Screening of common differentially expressed genes under three treatments

In 18 Masson pine samples, the majority of gene expression levels ranged from 0.0 to 1.0 (Fig. 3A). Differential gene analysis was conducted using a screening criteria of $\text{Padj} < 0.1$ and $|\log^2\text{FC}| \geq 1$. A total of 3014 differentially expressed genes were identified in the T25CK vs T25Z group, with 957 up-regulated and 2057 down-regulated genes detected (Additional File 2: Table S3). Similarly, in the T30CK vs T30Z group, a total of 4639 differentially expressed genes were found, including 1909 up-regulated and 2730 down-regulated genes

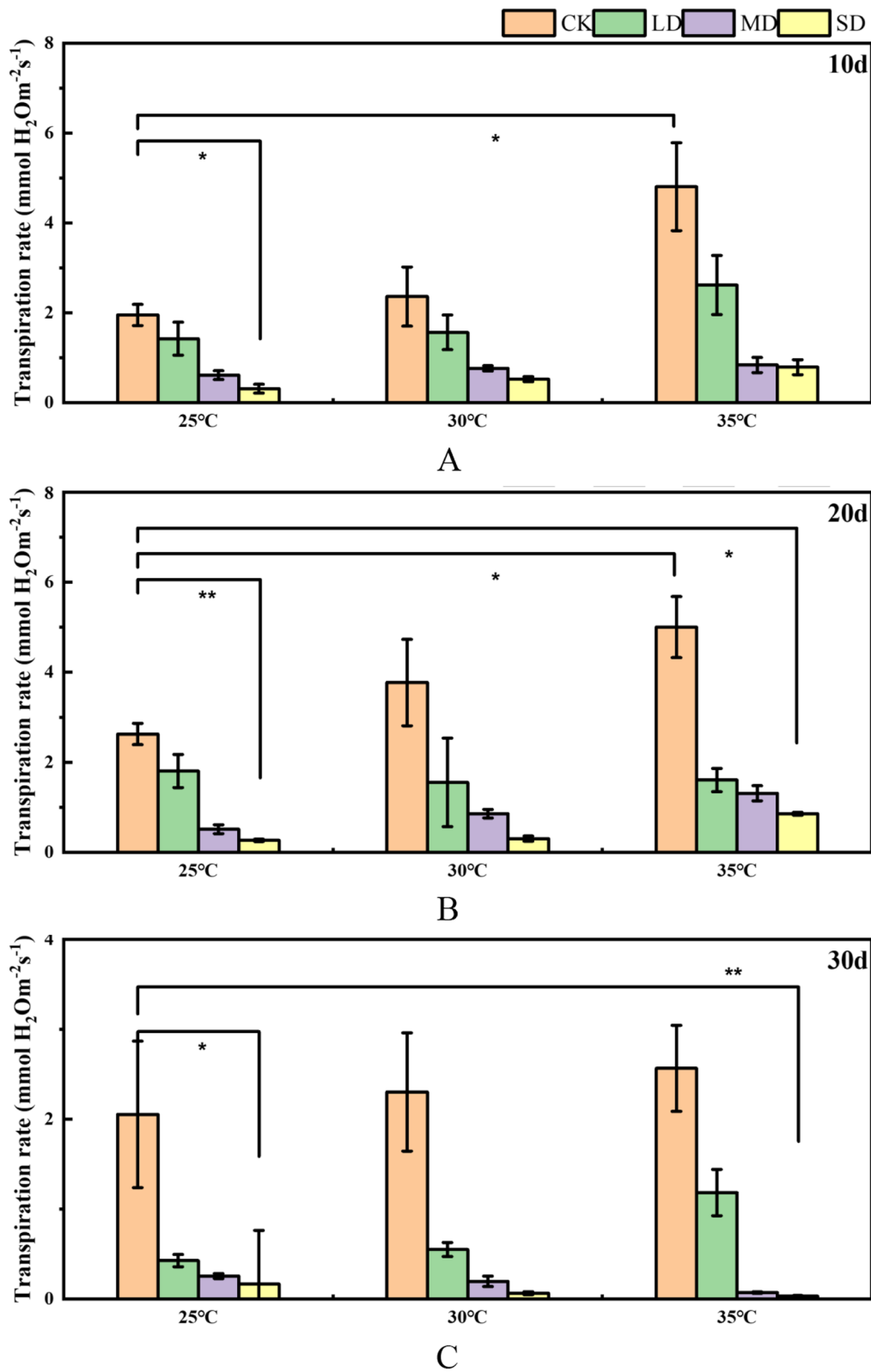


Fig. 2 Effects of high temperature and drought on the transpiration rate of Masson pine seedlings. The changes in transpiration rate after 10, 20, and 30 days of high temperature and drought stress are represented by Figure. **A, B, C** respectively. (* corresponds to the significance level of 5%, and ** corresponds to the significance level of 1%, CK: 75%-80% FC (field capacity), LD: 55%-60% FC, MD: 40%-45% FC, SD: 30%-35% FC)

Table 1 Quantity of transcriptome (Raw Reads: the overall count of original reads. Clean Reads: the number of high-quality sequence reads. Q20(%): the percentage of bases with a base recognition accuracy exceeding 99%. Q30(%): the percentage of bases with a base recognition accuracy exceeding 99.9%. The values 25, 30, and 35 correspond to temperatures of 25 °C, 30 °C, and 35 °C respectively, CK: 75%-80% FC, Z: 30%-35% FC)

Sample	Raw Reads	Clean Reads	Q20 (%)	Q30 (%)	Clean Reads %
T25CK1	40,651,082	38,348,600	98.1	94.38	94.33
T25CK2	40,160,896	37,924,222	98.16	94.45	94.43
T25CK3	38,639,068	36,433,556	98.12	94.43	94.29
T25Z1	36,949,042	34,832,706	98.12	94.45	94.27
T25Z2	46,602,818	43,923,726	98.22	94.68	94.25
T25Z3	42,352,046	39,865,744	98.3	94.9	94.12
T30CK1	39,152,846	36,920,674	98.23	94.67	94.29
T30CK2	39,230,734	37,041,144	98	94.12	94.41
T30CK3	40,692,646	38,429,136	98.08	94.31	94.43
T30Z1	45,105,096	42,492,918	98.26	94.73	94.2
T30Z2	45,225,782	42,609,752	97.85	93.77	94.21
T30Z3	45,419,054	42,799,492	98.16	94.52	94.23
T35CK1	39,756,730	37,510,860	98.07	94.32	94.35
T35CK2	44,912,260	42,351,116	97.98	94.07	94.29
T35CK3	44,009,176	41,485,354	97.97	94.07	94.26
T35Z1	42,802,754	40,300,800	98.13	94.44	94.15
T35Z2	41,423,928	38,982,238	98.2	94.63	94.1
T35Z3	43,440,540	40,852,800	98.2	94.62	94.04

(Additional File 3: Table S4). Furthermore, in the T35CK vs T35Z group, a total of 6632 differentially expressed genes were identified with an up-regulation count of 2781 and down-regulation count of 3851 (Additional File 4: Table S5) (Fig. 3B). By employing Venn diagrams for all three treatment groups' data comparison, a set of 1205 differentially expressed genes were discovered as co-expressed among them. (Fig. 3C).

KEGG enrichment analysis of differentially expressed genes under different treatments

The differentially expressed genes treated with T25CK vs T25Z, T30CK vs T30Z, and T35CK vs T35Z were subjected to KEGG enrichment analysis. Among the 3014 differentially expressed genes treated with T25CK vs T25Z, a total of 1106 genes were enriched. Among these, 335 genes were up-regulated while 700 genes were down-regulated. Among the 4639 differentially expressed genes treated with T30CK vs T30Z, a total of 1988 genes were found to be significantly enriched. Specifically, there were 792 up-regulated genes and 1039 down-regulated genes. Among the 6631 differentially expressed genes treated with T35CK vs T35Z, 2788 differentially expressed genes were enriched, of which 1218 were up-regulated and

1295 were down-regulated. KEGG enrichment analysis of transcriptome data from three different temperature and severe drought treatments for 30 days showed that 127, 134 and 137 metabolic pathways were enriched under T25CK vs T25Z, T30CK vs T30Z and T35CK vs T35Z, respectively (Additional File 5: Table S6, S7, S8). The enrichment analysis comparing T25CK and T25Z revealed a total of 13 carbon metabolic pathways. Among these, five pathways were found to be enriched with significant differences (P -value < 0.5): glycolysis/gluconeogenesis, galactose metabolism, starch and sucrose metabolism, pyruvate metabolism, and inositol phosphate metabolism. Starch and sucrose metabolism were enriched to a maximum of 53 differentially expressed genes (Fig. 4A)(Additional File 6: Table S9). The enrichment analysis comparing T30CK and T30Z revealed a total of 13 carbon metabolic pathways. Among these, six pathways were found to be enriched with significant differences (P -value < 0.5): glycolysis/gluconeogenesis, pyruvate metabolism, glyoxylate and dicarboxylate metabolism, pentose phosphate pathway, citrate cycle (TCA cycle) and ascorbate and aldarate metabolism. Starch and sucrose metabolism were enriched to a maximum of 68 differentially expressed genes (Fig. 4B) (Additional File 7: Table S10). The enrichment analysis comparing T35CK and T35Z revealed a total of 13 carbon metabolic pathways. Among these, ten pathways were found to be enriched with significant differences (P -value < 0.5): glyoxylate and dicarboxylate metabolism, starch and sucrose metabolism, citrate cycle (TCA cycle), pentose phosphate pathway, glycolysis/gluconeogenesis, fructose and mannose metabolism, propanoate metabolism, pyruvate metabolism, inositol phosphate metabolism and butanoate metabolism. Starch and sucrose metabolism were enriched to a maximum of 84 differentially expressed genes (Fig. 4C) (Additional File 8: Table S11).

Therefore, it is evident that the number of differentially expressed genes, carbon metabolic pathways enriched by these genes, and significantly enriched carbon metabolic pathways exhibit a gradual increase in response to escalating combined stress from high temperature and drought. The starch and sucrose metabolism exhibited the highest enrichment of differential metabolic genes among the three treatments, particularly evident in the T25CK vs T25Z and T35CK vs T35Z comparisons. Therefore, the starch and sucrose metabolism pathway emerges as the pivotal metabolic response of Masson pine seedlings to high temperature and drought stress.

The further analysis of differentially enriched metabolic genes involved in starch and sucrose metabolism across the three treatments revealed a total of 27 co-enriched genes, among which 9 were up-regulated and 15

Table 2 The statistics of RNASeq mapping. (Clean Reads: the total number of sequences used for alignment. Total_Mapped: compare the total number of sequences in the reference genome, the percentage represents the ratio of total mapped to clean reads. Multiple_Mapped: compare the total number of sequences to multiple locations, the percentage represents multiple mapped/total mapped. Uniquely_Mapped: the total number of sequences aligned to only one position, percentages represents uniquely mapped/total mapped. The values 25, 30, and 35 correspond to temperatures of 25 °C, 30 °C, and 35 °C respectively, CK: 75%-80% FC, Z: 30%-35% FC)

Sample	Clean_Reads	Total_Mapped	Multiple_Mapped	Uniquely_Mapped
T25CK1	38,348,600	29,976,384 (78.17%)	3,895,388 (12.99%)	26,080,996 (87.01%)
T25CK2	37,924,222	29,726,811 (78.38%)	3,839,436 (12.92%)	25,887,375 (87.08%)
T25CK3	36,433,556	28,328,324 (77.75%)	3,675,909 (12.98%)	24,652,415 (87.02%)
T25Z1	34,832,706	27,470,506 (78.86%)	3,497,848 (12.73%)	23,972,658 (87.27%)
T25Z2	43,923,726	34,416,797 (78.36%)	4,447,244 (12.92%)	29,969,553 (87.08%)
T25Z3	39,865,744	31,362,974 (78.67%)	3,944,800 (12.58%)	27,418,174 (87.42%)
T30CK1	36,920,674	28,845,654 (78.13%)	3,748,375 (12.99%)	25,097,279 (87.01%)
T30CK2	37,041,144	28,928,651 (78.10%)	3,749,472 (12.96%)	25,179,179 (87.04%)
T30CK3	38,429,136	29,851,865 (77.68%)	3,935,189 (13.18%)	25,916,676 (86.82%)
T30Z1	42,492,918	32,677,002 (76.90%)	4,098,846 (12.54%)	28,578,156 (87.46%)
T30Z2	42,609,752	32,250,497 (75.69%)	4,166,230 (12.92%)	28,084,267 (87.08%)
T30Z3	42,799,492	32,670,829 (76.33%)	4,230,763 (12.95%)	28,440,066 (87.05%)
T35CK1	37,510,860	28,752,738 (76.65%)	3,736,957 (13.00%)	25,015,781 (87.00%)
T35CK2	42,351,116	32,342,688 (76.37%)	4,174,159 (12.91%)	28,168,529 (87.09%)
T35CK3	41,485,354	31,715,253 (76.45%)	4,101,931 (12.93%)	27,613,322 (87.07%)
T35Z1	40,300,800	31,327,335 (77.73%)	4,374,634 (13.96%)	26,952,701 (86.04%)
T35Z2	38,982,238	30,043,717 (77.07%)	4,027,367 (13.41%)	26,016,350 (86.59%)
T35Z3	40,852,800	31,547,932 (77.22%)	4,704,806 (14.91%)	26,843,126 (85.09%)

were down-regulated simultaneously (Additional File 9: Table S12). The GO analysis of 27 common differentially expressed genes revealed that these genes were significantly enriched in the cellular component (GO:0005575), biological process (GO:0008150) and metabolic rate process (GO:0008152), catalytic activity (GO:0003824). The analysis revealed enrichment of 26 differentially expressed genes in the cellular component GO:0005623 (Fig. 5).

Common differential metabolite mining under different treatments.

Through the analysis of metabolome data from three different temperatures and severe drought treatment for 30 days, a total of 652 (Additional File 10: Table S13) distinct metabolites were identified using the OPLS-DA model (VIP > 1.0 and P value < 0.05). The principal component analysis (PCA) model effectively captured the sample variations, with PC1 and PC2 accounting for contribution rates of 20.3% and 11%, respectively (Fig. 6A). The samples exhibited consistent distribution patterns in distinct areas, indicating significant metabolic differences in Masson pine seedlings under hierarchical high temperature and drought conditions. A Venn diagram analysis revealed that there were 192 common differentially abundant metabolites across all three groups (Fig. 6B).

KEGG enrichment analysis of common differential metabolites

KEGG enrichment analysis was conducted on 192 (Additional File 11: Table S14) common differential metabolites obtained from three different treatments (Additional File 12: Table S15; Additional File 13: Table S16; Additional File 14: Table S17) (Fig. 7A). A total of 192 common differentially enriched metabolites were identified across 68 metabolic pathways (Additional File 15: Table S18). Among them, 6 carbon metabolic pathways were found to be enriched, including the pentose phosphate pathway, pentose and glucuronate interconversions, carbon fixation in photosynthetic organisms, starch and sucrose metabolism, galactose metabolism, and glycolysis/gluconeogenesis (Additional File 16: Table S19). Analysis of the network diagram revealed interactions between these metabolic pathways with overlapping enrichment of certain metabolites (Fig. 7B).

Based on the transcriptome data, it has been identified that starch and sucrose metabolism play a pivotal role in the response of Masson Pine seedlings to the combined stress of high temperature and drought. Further analysis of metabolites enriched by starch and sucrose metabolism in the metabolome reveals

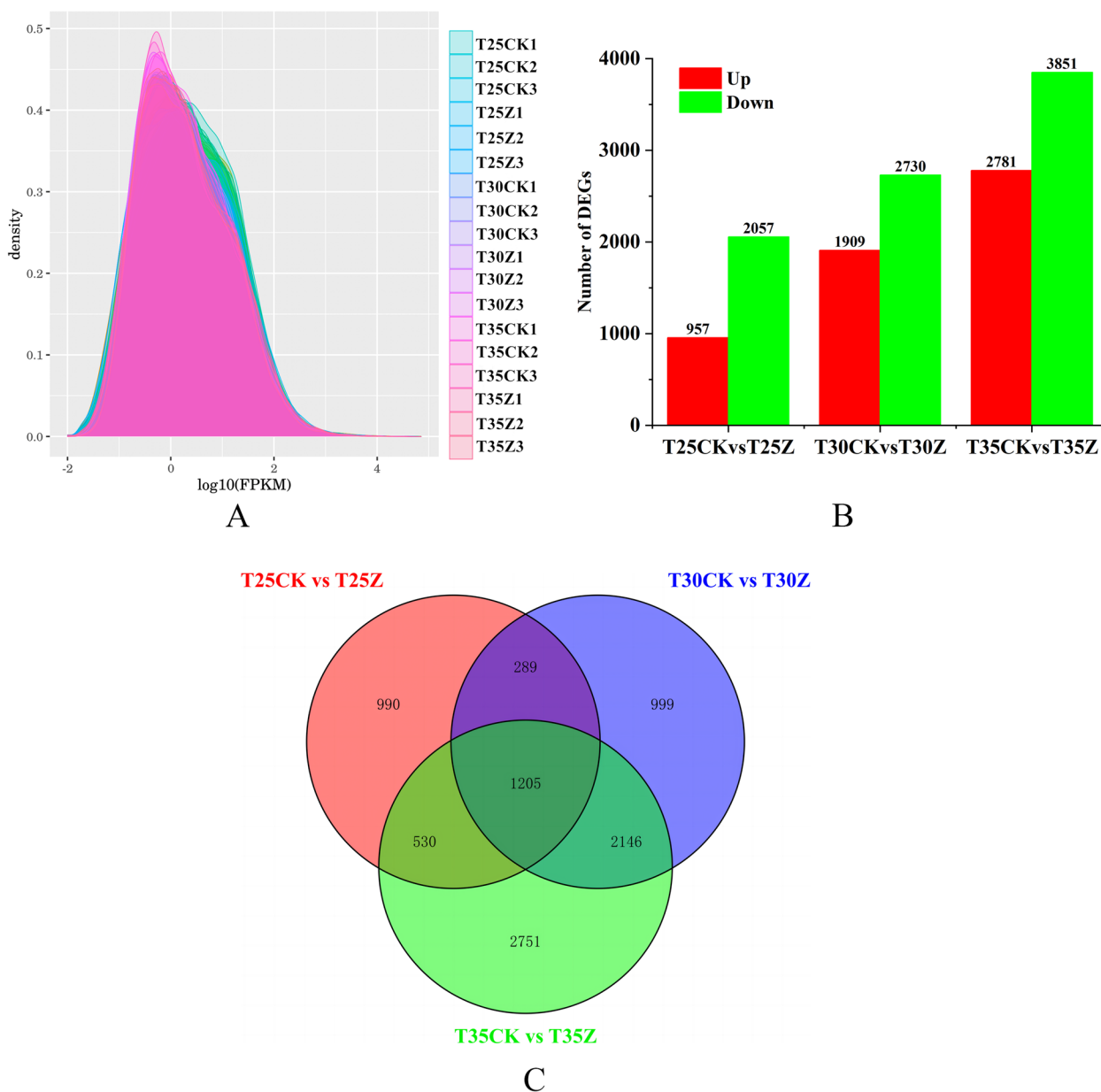


Fig. 3 Differentially expressed genes of Masson pine under different treatments (**A**: The distribution of FPKM (Fragments Per Kilo bases per Million fragments) density; **B**: The number of differentially expressed genes under different treatments; **C**: Venn diagram for three treatments, The values 25, 30, and 35 correspond to temperatures of 25 °C, 30 °C, and 35 °C respectively, CK: 75%-80% FC, Z: 30%-35% FC)

only two distinct metabolites accumulated: Galactose 1-phosphate (C00103) and Trehalose (C01083).

Combined transcriptome and metabolome analysis of starch and sucrose metabolic

The differential metabolites and transcriptomic differentially expressed genes of T25CK vs T25Z, T30CK vs T30Z, and T35CK vs T35Z were simultaneously mapped to the pathways of starch and

sucrose metabolism for integrated analysis, aiming to elucidate the intricate relationship between genes and metabolites in these metabolic processes (Additional File 17: Table S20). With T25CK vs T25Z, the elevated levels of trehalose and trehalose 6 phosphate were due to the up-regulated expression of *PmTPS1* and *PmTPS5* genes. The significant increase in glucose 1-phosphate may be attributed to the up-regulation of phosphoglucomutase [EC:5.4.2.2] and phosphate

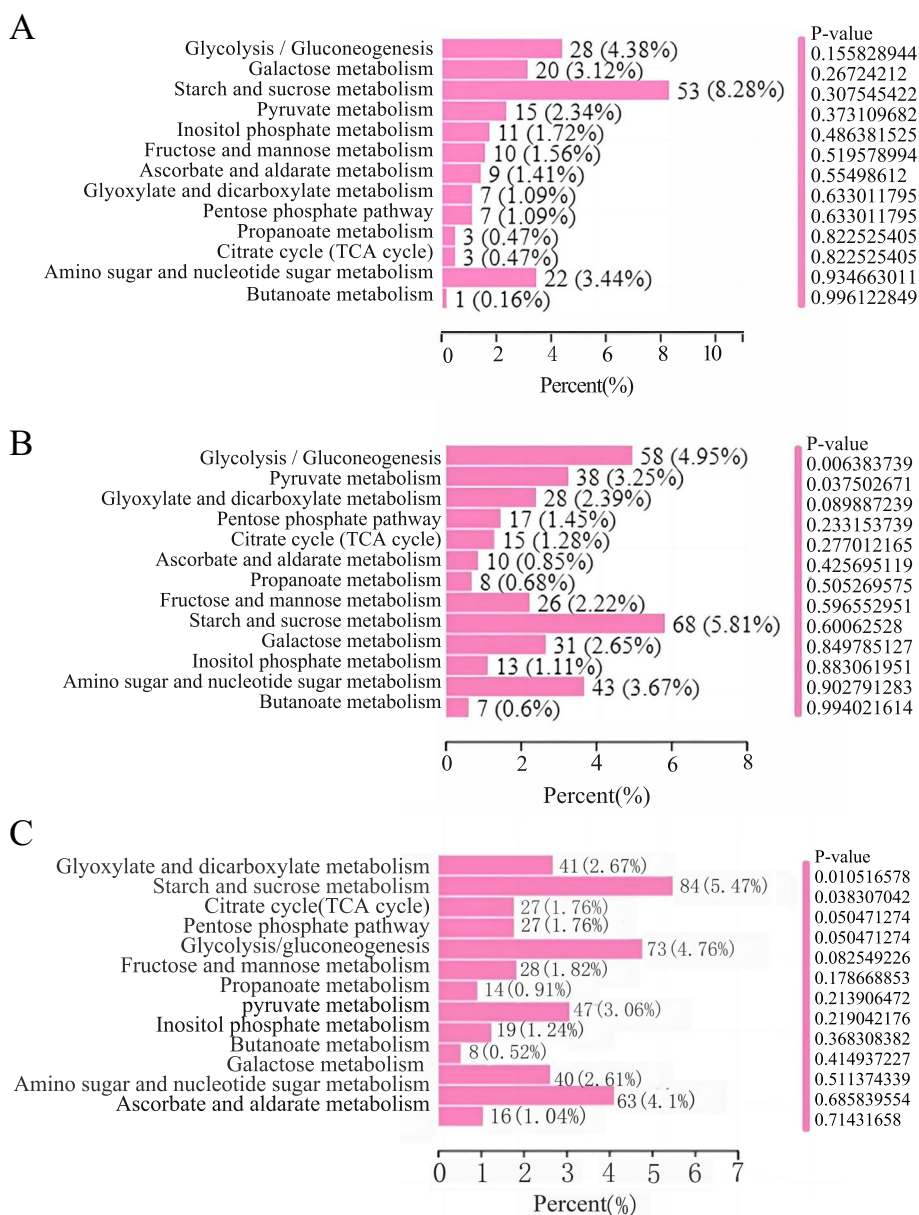


Fig. 4 Advanced KEGG classification histogram of carbon metabolism of Masson pine seedlings under three treatments. **A:** T25CK vs T25Z; **B:** T30CK vs T30Z; **C:** T35CK vs T35Z. Percent (%). The number of metabolites with significant differences annotated in this pathway accounted for the proportion of metabolites with significant differences annotated capitalize KEGG, CK: 75%-80% FC, Z: 30%-35% FC

adenylyltransferase [EC:2.7.7.27] which is caused by the downregulation of the gene (Additional File 18: Fig. S3). The increase in trehalose content observed in the T30CK vs T30Z comparison can be attributed to the up-regulated expression of *PmTPS5* and *PmTPS1* genes. However, there was no significant increase in trehalose 6-phosphate (Additional File 18: Fig. S4). The increase in trehalose content with T35CK vs T35Z was attributed to the upregulated expression of *PmTPS5*, *PmTPS1*, and *PmTPPD* genes (Additional File 18: Fig.

S5). In summary, among the three treatments of T25CK vs T25Z, T30CK vs T30Z and T35CK vs T35Z, only trehalose exhibited an upward trend. Therefore, trehalose is the core metabolite of Masson pine seedlings in response to high temperature and drought. The differentially expressed genes co-enriched under the three treatments included *PmTPS5* and *PmTPS1*.

To further validate the correlation between genes and metabolites, a heat map of trehalose metabolism was constructed, revealing that only *PmTPS5* and trehalose

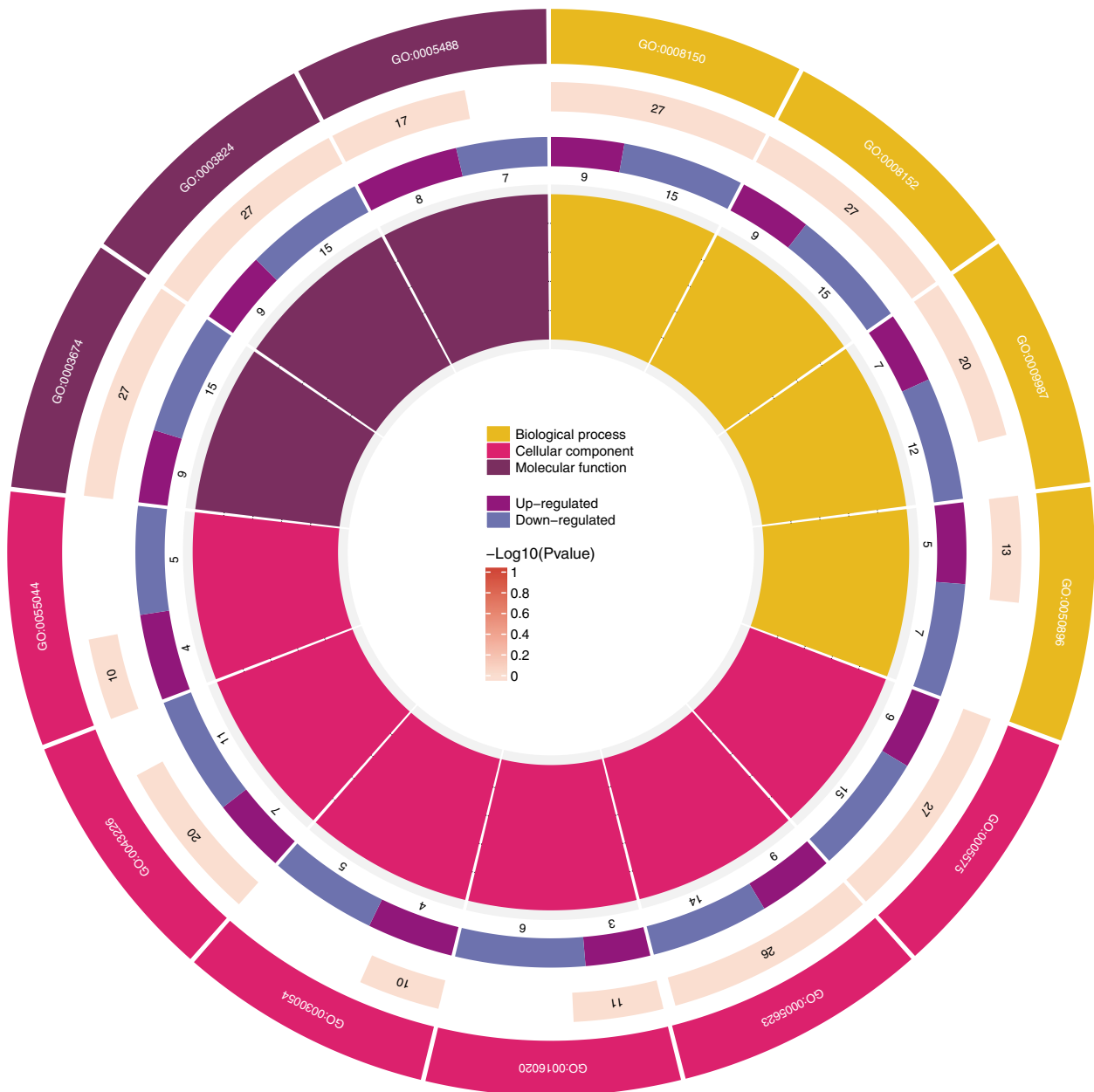
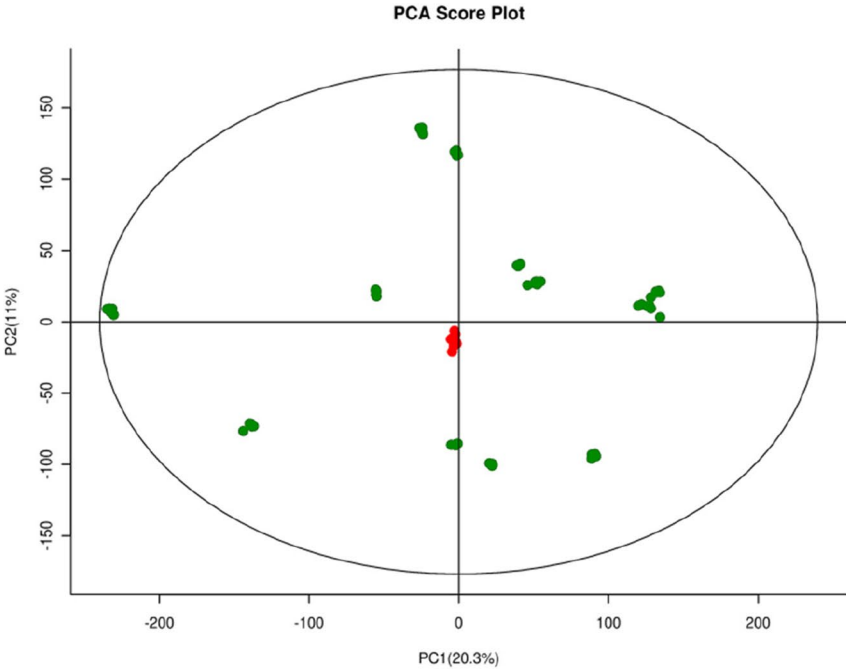


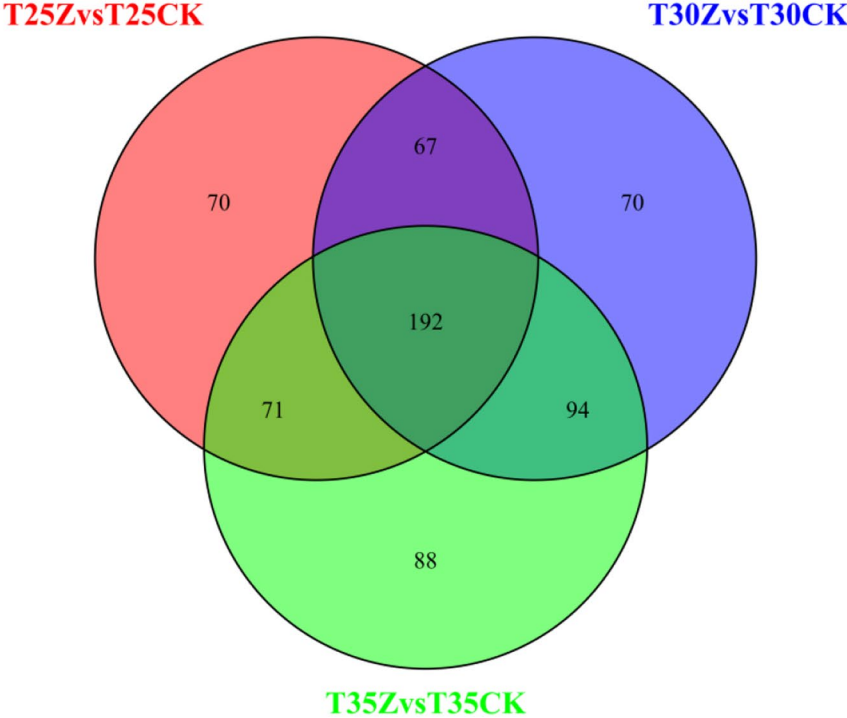
Fig. 5 The GO enrichment analysis of 27 commonly differentially expressed genes is visualized as a circular plot, where the outermost circle represents gene ontology terms, the second circle depicts the total number of genes associated with each term using color-coded $-\log_{10}(P\text{-value})$, the third circle indicates the number of up- and down-regulated genes, the fourth circle represents Rich factor, and finally, the innermost circle provides legend information

exhibited consistent changes among the common differentially expressed genes across all three treatments (Fig. 8). Compared with T25CK vs T25Z, the gene *PmT-PPD* was more enriched under T35CK vs T35Z treatment, which aligns with the trend observed for trehalose. Therefore, the *PmTPS1*, *PmTPS5* and *PmTPPD* genes

serve as pivotal regulatory genes in Masson Pine seedlings' response to high temperature and drought stress. The regulation primarily involves the upregulation of gene expression, resulting in increased trehalose synthase activity and the accumulation of a substantial amount of trehalose to enhance Masson pine's resistance to high temperatures and drought.

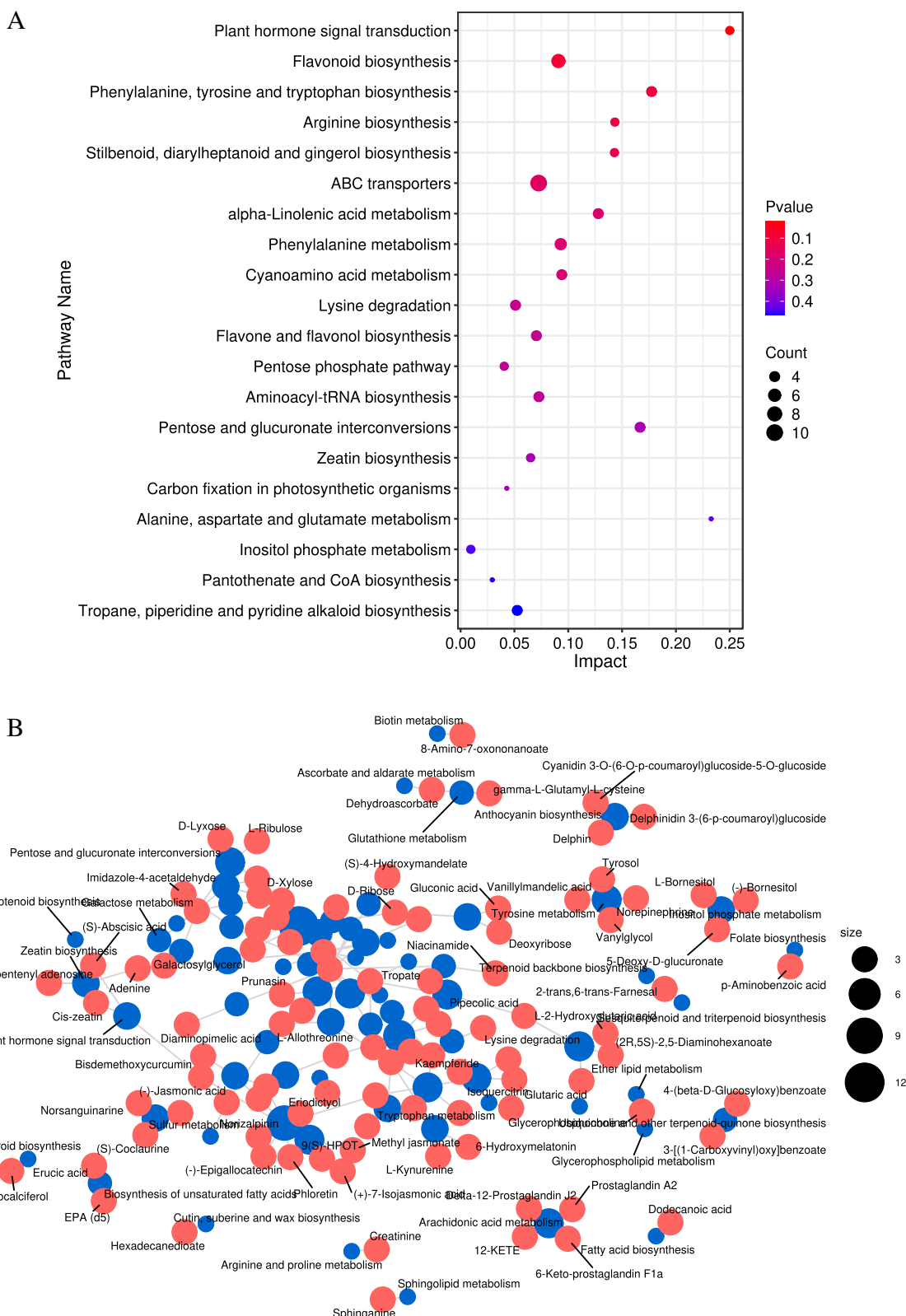


A



B

Fig. 6 PCA analysis (A) and differential metabolite Venn diagram (B) in Masson pine (The values 25, 30, and 35 correspond to temperatures of 25 °C, 30 °C, and 35 °C respectively, CK: 75%-80% FC, Z: 30%-35% FC)



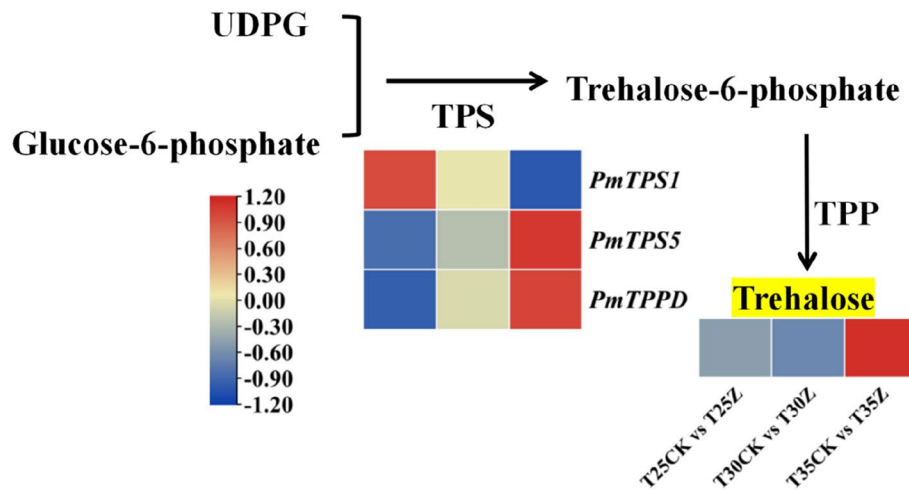


Fig. 8 Metabolic pathway map of differentially expressed genes and Trehalose, the heat map illustrates the alteration in the disparity ratio of gene, trehalose across three temperature treatments, CK: 75%-80% FC, Z: 30%-35% FC. The values 25, 30, and 35 correspond to temperatures of 25 °C, 30 °C, and 35 °C respectively

Analysis of qRT-PCR expression of differentially expressed genes

To verify the reliability of transcriptome data, qRT-PCR was performed on the selected core regulatory genes *PmTPS1*, *PmTPS5* and *PmTPPD*. As shown in Fig. 9, the expression trends of the three genes were generally

consistent with the results of the transcriptome data, indicating that the results of the transcriptome data were reliable. It can be preliminarily concluded that the above three genes are the core regulatory genes of carbon metabolism of Masson Pine seedlings in response to high temperature and drought.

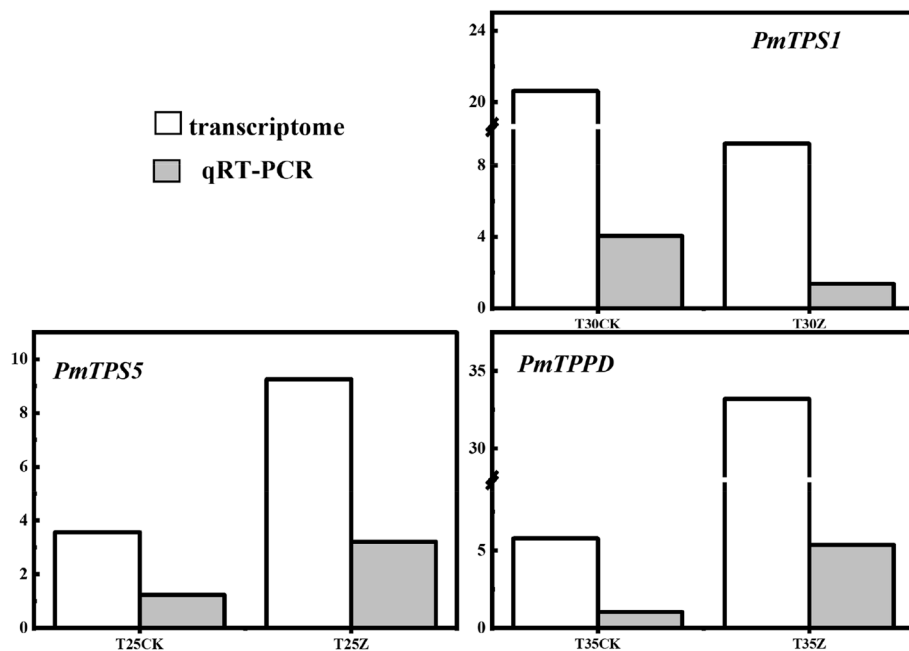


Fig. 9 qRT-PCR map of core genes, The relative expression levels were employed for qRT-PCR analysis, while FPKM values were utilized for transcriptomics investigation, CK: 75%-80% FC, Z: 30%-35% FC. The values 25, 30, and 35 correspond to temperatures of 25 °C, 30 °C, and 35 °C respectively

Discussion

Effects of high temperature and drought on photosynthetic carbon metabolism of plants

As one of the most crucial physiological processes in the plant kingdom, photosynthesis is primarily influenced by stomatal conductance, mesophyll conductance, and enzymatic biochemistry [19]. Plants perceive drought through their roots, and when it surpasses a certain threshold, leaf stomata close to minimize water loss [20, 21]. The intensification of high-temperature weather will further elevate the Vapor Pressure Deficit (VPD) in the atmosphere, subsequently reducing stomatal conductance and exacerbating drought conditions. Research has revealed that drought initially hampers plant growth followed by a decline in photosynthesis; meanwhile, respiration may decrease due to restricted growth metabolism or substrate limitations [22]. Transpiration serves as an essential mechanism for plants to mitigate heat-induced damage [23]. It has been observed that with increasing temperature, there is a transition from stomatal opening to closure [24]. Besides temperature regulation, the influence of vapor pressure deficit (VPD) is equally crucial, and stomatal transport determines the diffusion capacity of carbon dioxide [25]. Stomatal conductance has emerged as a key limiting factor for plant photosynthesis. Moreover, high temperatures and drought also impact the activity of ribulose-1, 5-diphosphate carboxylase/oxygenase (Rubisco), which serves as a light- and carbon-fixing enzyme [26]. The effect of drought on Rubisco remains controversial due to variations in intensity and duration [27–29], while high temperatures primarily weaken the activity of Rubisco's catalytic companion, Rubisco activating enzyme [30, 31]. This experiment aligns with previous studies by demonstrating that under similar temperatures, both the photosynthetic rate and transpiration rate of Masson Pine seedlings gradually decrease with increasing levels of drought. In particular, the impact of high temperature and drought stress on the photosynthetic rate of Masson Pine seedlings was more pronounced compared to either drought or high-temperature stress alone. During the initial stages of high-temperature treatment and under mild to moderate drought conditions, there was a certain degree of increase in transpiration rate; however, as stress intensified, a significant decrease in final transpiration rate was observed. This phenomenon is likely attributed to the presence of abundant substrates in Masson Pine leaves during the early stages of stress. Additionally, it is possible that increasing temperatures may lead to an upregulation in photosynthetic enzyme activity. Therefore, determining whether the substantial decline in photosynthetic and transpiration rates among Masson Pine seedlings is primarily caused by reduced light availability and

related enzyme activities or by decreased stomatal conductance influenced by hormones will be one crucial area for future research.

Effects of high temperature and drought on plant carbon catabolism

Glucose metabolism not only provides energy and carbon skeletons for plant development, but also serves as signaling molecules and metabolites to regulate responses to abiotic stresses [32]. Studies have revealed that plants exposed to high temperatures and drought stress generate a substantial amount of reactive oxygen species (ROS) and free radicals, resulting in oxidative damage to DNA, proteins, and lipids [33]. In severe cases, this leads to programmed cell death in plants [34]. Glucose metabolism plays a crucial role in preventing programmed cell death by eliminating reactive oxygen species from plants [35]. Simultaneously, the energy produced through glucose metabolism promotes the pentose phosphate pathway, generating antioxidant substances that further eliminate reactive oxygen species to safeguard plant cells [36]. This conclusion has been substantiated by studies conducted on *Soybeans* [36], *Arabidopsis* [37], and *Potato* [38].

In addition, high concentrations of certain monosaccharides such as fructan can serve as active oxygen scavengers [39], suggesting that sugar metabolism may protect plant cells from reactive oxygen species during periods of high temperature and drought stress. It has also been discovered that promoting the biosynthesis of heat shock proteins is another way to mitigate damage caused by high temperatures and drought on plants [40]. In this study, transcriptome and metabolome analyses were conducted on Masson pine seedlings subjected to high temperature and drought stress, revealing sucrose and starch metabolism pathways as core metabolic pathways in response to these conditions. This finding is consistent with previous studies on glucose metabolism under similar stresses. Further analysis revealed trehalose's central role in sugar metabolism for Masson pine, with no precursor substances such as sucrose or starch detected. This may be due to the severe drought conditions used in this study where cells had almost completely lost water; trehalose acts as an osmoprotector protecting proteins and cell membranes while allowing for full recovery after rehydration [17, 18]. Whether trehalose or precursor substances like sucrose or starch are more important under mild or light drought requires further research.

Effects of high temperature and drought on trehalose metabolism in plants.

Trehalose, a non-reductive disaccharide, is widely present in living organisms. It not only provides energy for plants but also serves as a protective agent for

membrane proteins [41]. Because of the very stable nature of trehalose, it plays an important role in protecting the stability of plant membrane proteins under stress such as high temperature and drought [42]. Therefore, although the content of trehalose is low, it plays an irreplaceable protective role. Studies have found that to enhance the ability to resist drought stress, *Selaginella* accumulates a large amount of trehalose in its body [43, 44]. Under heat shock and cold treatment, the trehalose content of *Arabidopsis* increased by 1 and 8 times, respectively [45]. Under drought stress, it was found that trehalose played a major role in resisting drought stress, rather than starch and sucrose and other prerequisite substances [46].

This study also revealed that trehalose, rather than starch and sucrose, was identified as the key substance in Masson pine seedlings for withstanding high temperature and drought stress. Further investigation is required to determine whether the prolonged duration of severe drought stress contributes to this finding. Moreover, exogenous addition of trehalose not only enhances plant resistance but also improves photosynthesis and activates oxygen scavenging enzymes. Previous studies have demonstrated that exogenous trehalose primarily enhances plant stress resistance by increasing maximum photosynthetic efficiency and electron transfer rate of PSII [47]. Additionally, circulating electron flow and plastoquinone pool can alleviate photoinhibition [48]. Similarly, further research and verification are needed to ascertain whether exogenous trehalose can enhance the ability of Masson pine seedlings to withstand high temperatures and drought.

In the trehalose metabolic pathway, TPS and TPP play a crucial regulatory role (Fig. 10). The verification of TPS and TPP gene overexpression in various plant species has significantly enhanced their drought resistance. For instance, the transfer of cassava's *MeTPS1* gene into tobacco resulted in transgenic tobacco plants accumulating substantial amounts of trehalose, thereby greatly improving their drought tolerance [46]. Transgenic rice plants with *OsTPS1* [49] and *OsTPP3* [50] genes exhibited increased resistance to drought conditions and higher trehalose content [49]. Overexpression of *AtTPPB*, *AtTPPE*, activation of *AtTPPF* transcription [51], *AtTPPI* [52], as well as overexpression of wheat *TaTPP7*

gene [53], substantially improved drought resistance in *Arabidopsis Thaliana* by reducing stomatal pore size and enhancing root configuration for improved water use efficiency. This study also revealed that TPS and TPP genes maintained high expression levels during stress treatment through joint transcriptome and metabolome analysis, consistent with previous research findings. It is speculated that the upregulation of TPS and TPP-related genes may be responsible for responding to combined stresses from high temperature and drought in Masson Pine seedlings. The increased enzyme activities of TPS and TPP further promoted trehalose accumulation; however, further research is needed to determine if these enzyme activities are indeed increased. Additionally, investigating whether trehalose accumulation caused by interaction between drought stress and high temperatures affects stomatal changes or alterations in root structure will be a key focus for future studies.

Conclusions

In this study, the response mechanism of Masson pine seedlings to stress was studied for the first time by cross-stress of high temperature and drought. The results showed that, compared with the single stress of high temperature or drought, the effects of high temperature and drought on photosynthetic rate, transpiration rate, transcriptome and metabolome were more significant. The analysis of transcriptome data revealed that the carbon metabolism pathway of Masson Pine seedlings was affected by both high temperature and drought stress. The metabolome analysis revealed that only trehalose and Galactose 1-phosphate were specifically associated with the starch and sucrose metabolic pathways. Among these comparison groups, only trehalose exhibited significant upregulation. Trehalose along with *PmTPS1*, *PmTPS5*, and *PmTPPD* genes played crucial roles as metabolites and key regulators within the starch and sucrose metabolism.

Material and methods

Plant materials and growth conditions

The experiment was conducted in the nursery base of Guizhou University. The plant pot has a diameter of 300 nm, a lower diameter of 200 nm and a height of 250 nm. The soil was rhizosphere loess under the Masson

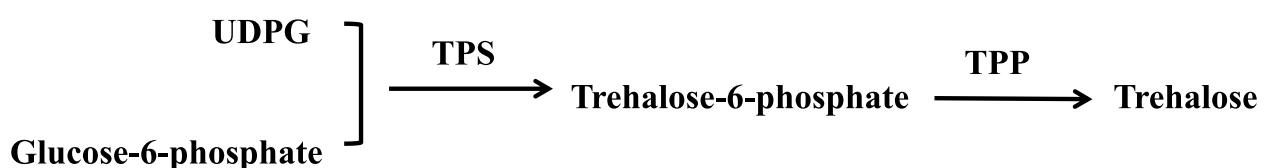


Fig. 10 Synthesis pathway of trehalose in plants

pine forest, and the same weight of soil was placed in each pot. Before the experiment, the seedlings of Masson pine were maintained normally for 3 months. Finally, 200 seedlings with the same growth trend were selected for the hierarchical high temperature and drought experiment.

High temperature and drought treatment

The split zone test method was employed in this study, with the main zone temperature divided into three zones: 25/25°C, 30/25°C, and 35/25°C. The time was set to 16h/8h for day and night, respectively. The daytime temperature and duration of the three primary zones are set at 25°C, 30°C, and 35°C respectively, spanning from 6:00 to 22:00; whereas the evening temperature remains constant at 25°C during the period from 22:00 to 6:00. Four groups of water stress were set in each main zone, as follows: based on the relative water content of the soil, three drought gradients were set at 30%-35% field capacity (FC) (severe drought, SD), 40%-45% FC (moderate drought, MD), 55%-60% FC (mild drought, LD), respectively. and 75%-80% FC (control, CK). Repeat 10 POTS per treatment and plant 1 plant per pot. The relative water content of the soil was maintained by the weighing method. Samples were taken at 10-day intervals. Irradiance is 400–450 μmolm⁻² s⁻¹ PAR. The relative humidity is 40%-50% in light and 70%-80% in darkness. The specific sampling time is shown in Table 3.

Photosynthesis and stomatal conductance measurements

Leaf photosynthetic rate and stomata conductance were measured using a portable open gas exchange system (Li-6400XT, Li-Cor, Lincoln, NE, USA) equipped with the red and blue light source (6400-2B) from 9:00 am to 11:00 am. Needle photosynthetic rate under saturating light (Asat, μmol m⁻² s⁻¹), stomatal conductance (Gs, mol m⁻² s⁻¹), and transpiration rate (E, mmol m⁻² s⁻¹) were measured under the following conditions: photosynthetically active radiation of 1200 μmol m⁻² s⁻¹, [CO₂] of 400 μmol mol⁻¹, and flow rate of 500 mmol s⁻¹. Each

Table 3 Sampling time for high temperature and drought treatment

Temperature	25°C/30°C/35°C			
	CK	LD	MD	SD
Time gradient				
10d	a	a	a	a
20d	a	a	a	a
30d	a	a	a	a

^a is the sampling point, CK: 75%-80% FC (field capacity), LD: 55%-60% FC, MD: 40%-45% FC, SD: 30%-35% FC.

group underwent five measurements, and the three most consistent data points were chosen for further analysis.

The determination and analysis of the transcriptome of Masson pine

The preparation of transcriptome samples

For each treatment, control and severe drought treatment were selected for 30 days for transcriptome determination. The transcriptome sampling method was conducted as follows: The upper portion of the leaves from all treated Masson pine seedlings were collected. The six plants exhibiting similar growth were carefully selected for each treatment and assigned numbers 1 to 6. Plant 1 and 2, plant 3 and 4, as well as plant 5 and 6 were combined, thoroughly mixed, promptly frozen in liquid nitrogen, and subsequently ground into a fine powder. This process resulted in three samples for each treatment. Considering there were six treatments with three replicates per treatment, a total of eighteen samples were obtained. The corresponding numbers are 25 °C CK and severe drought (T25CK vs T25Z), respectively. 30 °C CK and severe drought (T30CK vs T30Z) and 35 °C CK and severe drought (T35CK vs T35Z). RNA was extracted by the extraction kit DP441 (TIANGEN BIOTECH (BEIJING)CO., LTD.) and then reverse-transcribed (Thermo Scientific NanoDrop 2000). Qualified samples were sent to Suzhou Panomick Biopharmaceutical Technology Co., Ltd for sequencing. The result is high-quality clean data.

The experimental procedure specific to RNASeq

The mRNA containing a polyA structure in the total RNA sample was selectively enriched using Oligo(dT) magnetic beads, followed by fragmentation of the RNA into approximately 300 bp fragments through ion interruption. The first cDNA strand was synthesized using RNA as a template, employing 6-base random primers and reverse transcriptase. Subsequently, the second cDNA strand was synthesized utilizing the first cDNA strand as a template to accomplish library construction. After the completion of library construction, PCR amplification was employed to enrich the library fragments, followed by library selection based on fragment size, resulting in a final library size of 450 bp. The library was subsequently subjected to inspection using the Agilent 2100 Bioanalyzer, wherein the total concentration and effective concentration of the library were determined. The libraries containing different Index sequences are mixed proportionally based on the effective concentration of the library and the required amount of data, allowing each sample to be distinguished according to its respective Index. The hybrid library was uniformly diluted to a concentration of 2 nM, and the single strand

Table 4 Reference genome information

Genome	Pita.2_01.fa
Genebuild by	https://treegenesdb.org/FTP/Genomes/Pita/v2.01/
Base Pairs	22,104,357,184

library was generated through alkali denaturation. After performing RNA extraction, purification, and library construction procedures, the libraries were subjected to Paired-end (PE) sequencing using Next-Generation Sequencing (NGS) technology based on the Illumina HiSeq sequencing platform.

The whole genome of Masson pine has not yet been sequenced; therefore, reference transcriptome sequencing was employed in this experiment to ensure the accuracy of the sequencing results. The chosen reference species was *Pinus taeda* L., which is closely related to Masson pine. Detailed information regarding the reference genome can be found in Table 4.

The process of reference transcriptome analysis follows a specific protocol

The initial step involves filtering the raw data, followed by a comparison of the filtered clean data with the reference genome of the species. The expression levels of each gene were calculated based on the comparison results, and subsequent analyses including expression difference analysis, enrichment analysis, and cluster analysis were conducted for the samples. The transcription sequence was reconstructed through the process of splicing the aforementioned reads.

Refined data compilation, screening, and quality evaluation

After the samples are sequenced on the computer, image files are obtained and subsequently processed using the built-in software of the sequencing platform to generate FASTQ Raw Data. The Raw Data for each sample was individually tallied, encompassing the sample name, Q30 score, percentage of ambiguous bases, as well as Q20 (%) and Q30 (%). The presence of low-quality reads with junctions in the sequencing data necessitated further filtration to mitigate their significant interference on subsequent information analysis. The quality of a specific location was assessed by utilizing the single base mass distribution map derived from the sequencing data. The base content distribution is utilized for the detection of AT and GC separation, while the average mass distribution of reads is primarily employed to identify the sequencing data's average mass distribution.

The process of comparing and analyzing with a reference genome

The reference genome index was established using Bowtie2, followed by alignment of the filtered reads to the reference genome using Tophat2. The default settings for Reads and reference genome sequence Mismatch during TopHat comparison ensure a successful mapping, with a maximum allowable difference of two.

The analysis of expressions

The HTSeq tool was utilized to perform a statistical comparison of the Read Count value for each gene, representing the gene's original expression. The reads count exhibited a positive correlation with the true gene expression level, gene length, and sequencing depth. In order to ensure comparability of gene expression levels across different genes and samples, FPKM was employed for normalization of expression levels. FPKM represents the number of gene fragments per thousand base length per million fragments. For paired-end sequencing, two reads are generated from each fragment. FPKM exclusively considers the count of fragments derived from two reads that can be compared against the same transcript. The prevailing consensus among reference transcriptomes is that genes with $FPKM > 1$ are generally considered to be expressed. The FPKM density distribution allows for the comprehensive investigation of gene expression patterns across the entire sample. Typically, a majority of genes exhibit moderate expression levels, while only a small fraction display either low or high expression. The RSeQC tool was utilized to analyze the expression saturation, specifically at sampling ratios of 5%, 10%, 15%...100% in relation to the sequencing results. The gene expression levels were separately calculated for each gene with a total of 20 measurements, corresponding to different sampling ratios. These values were then compared against the actual expression level (assuming it was obtained under complete sampling) in order to determine the relative error. The primary objective of saturation analysis is to evaluate whether the available data is sufficient for accurate calculation of gene expression. The Principal Components Analysis (PCA) technique reduces the dimensionality of high-dimensional data to two or three dimensions using linear transformations, while preserving the most significant contributions from each variable, thereby simplifying data complexity. In cases where multiple samples are available, PCA is performed on each sample based on their expression levels using the DESeq software package in R language. This analysis enables grouping of similar samples together, with closer distances indicating higher similarity between samples.

Screening and Enrichment Analysis of differentially expressed genes.

Table 5 Primer sequences for real time PCR

Gene name	Forward primer (5'-3')	Reverse primer (5'-3')
<i>PmTPS1</i>	AGAAGGAGGCTTTGTTTG GTG	GAAGCAATCCGAGGAGT GTG
<i>PmTPS5</i>	CCCTCGTCTCCCTTACTCTT	TCAACAAAACACCAAGTCCA
<i>PmTPPD</i>	CCCTTGCTTTCATTTTCATT	GGCTAACACGATTCTCAACA
<i>UBC</i>	GATTATTTCATTGGCAGGC	AGGATCATCAGGATTTGGGT

The DESeq software was utilized to analyze the differential gene expression between T25CK and T25Z, T30CK and T30Z, as well as T35CK and T35Z within each group. The criteria for identifying differentially expressed genes were set as follows: $|\log_2FC| > 1$ & $\text{padj} < 0.1$. The KEGG enrichment results of differentially expressed genes were evaluated based on the Rich factor, FDR value, and the number of genes enriched in each pathway [54]. The enriched carbon metabolic pathways should be selected for visualization, followed by the identification of core metabolic pathways and genes that are enriched in relation to carbon metabolism.

qRT-PCR analysis

The primers used in this study were shown in Table 5, among which *UBC* was used as the internal reference primers. The primers were synthesized by Beijing Qingke Biotechnology Co., LTD. Quantitative real-time PCR was amplified by PCR with ABI 7300 fluorescence quantitative PCR instrument (USA), and each test was repeated 3 times. The reaction system is based on ChamQ SYBR Color qPCR Master Mix (2X) (Nanjing Novozan Biotechnology Co., Ltd.). The data are calculated by the $2^{-\Delta\Delta Ct}$ method [55].

The determination and analysis of the metabolome of masson pine

The preparation of metabolome samples

For each treatment, control and severe drought treatment were selected for 30 days for metabolome determination. The metabolome sampling method was conducted as follows: The upper portion of the leaves from all treated Masson pine seedlings were collected. The plants were sequentially labeled from 1 to 10 for each treatment. Plant 1 and 2, plant 3 and 4, plant 5 and 6, plant 7 and 8, plant 9 and 10 as well as plant 1–10 were combined, thoroughly mixed, promptly frozen in liquid nitrogen, and subsequently ground into a fine powder. This process resulted in six samples for each treatment. Considering there were six treatments with six replicates per treatment, a total of 36 samples were obtained. Subsequently, these samples were shipped to Suzhou Panomick Biopharmaceutical Technology Co., Ltd for metabolome while

being protected by dry ice. The corresponding numbers were the same as the transcriptome.

The determination and analysis of the metabolome.

An appropriate amount of samples were added into the centrifuge tube with methanol in advance, and after sufficient extraction, grinding and centrifugation, LC–MS detection was performed through a 0.22 μm filter membrane. LC uses the Vanquish UHPLC System (Thermo Fisher Scientific, USA). Chromatography was carried out with an ACQUITY UPLC[®] HSS T3 (150 \times 2.1 mm, 1.8 μm) (Waters, Milford, MA, USA). Two scanning modes, positive ion and negative ion, were used to collect MS signals. Data analysis software Progenesis QI (Waters Corporation, Milford, USA).

The MSConvert tool within the Proteowizard package (v3.0.8789) facilitates the conversion of the original mass spectrometry file into the mzXML file format. The RXCMS software package was utilized for peak detection, peak filtering, and peak alignment processing in order to obtain the substance quantification list. The parameters were set as follows: $\text{bw} = 2$, $\text{ppm} = 15$, $\text{peakwidth} = c(5, 30)$, $\text{mzwid} = 0.015$, $\text{mzdiff} = 0.01$, $\text{method} = \text{'centWave'}$. The following public databases were utilized for substance identification: HMDB, massbank, LipidMaps, mzcloud, KEGG, and a self-built material bank. The parameters were set at $\text{ppm} < 30$ ppm. The LOESS signal correction method, based on QC sample, achieves data correction and eliminates system errors. It filters out $\text{RSD} > \text{in QC}$ samples during data quality control, accounting for 30% of the total.

The R software package Ropls was utilized for conducting principal component analysis (PCA), partial least squares discriminant analysis (PLS-DA), and orthogonal partial least squares discriminant analysis (OPLS-DA) to reduce the dimensionality of the sample data. The data were normalized, and individual plots for score, load, and Splot were generated to visually represent the variations in metabolite composition among samples. The model's overfitting test was conducted using the permutation test method. The interpretation rates of the built model to the X and Y matrix are represented by R2X and R2Y respectively, while Q2 indicates the predictive ability of the model. The closer their values are to 1, the higher the degree of fit of the model, indicating a more accurate division of samples in the training set according to their original attributes. The P value was calculated using a statistical test, while the projected importance of variables (VIP) was determined through OPLS-DA dimensionality reduction method. Additionally, the difference multiple between groups was computed via fold change (FC). The influence strength and interpretation ability of each metabolite component content on sample classification and discrimination were evaluated to assist in the

screening of metabolites. The metabolite molecules were deemed statistically significant when the P value was less than 0.05 and the VIP score exceeded 1. The overlapping metabolites among the three treatments were analyzed using a Venn diagram. The MetaboAnalyst software package was utilized to perform functional pathway enrichment and topological analysis of the metabolites co-enriched among the three treatment groups. Subsequently, KEGG Mapper visualization tool was employed to scan enriched pathways for differential metabolites and pathway maps.

Based on the key metabolic pathways identified from the early transcriptome analysis and their corresponding metabolomic profiles, a heat map of the trehalose metabolic pathway was constructed to visualize the enrichment of genes and metabolites within this pathway. This approach aims to elucidate the correlation between metabolites and differentially expressed genes, ultimately leading to the identification of core regulatory genes and metabolites.

Statistical analysis

All assays were repeated at least 3 times, and the data were expressed as mean \pm SD. Statistical differences were measured using Duncan's test at the $p=0.05$ level. Data processing was conducted with Microsoft Excel 2010. Line and column charts were drawn by Origin 2021. The Venn diagram and KEGG enrichment analysis diagram were performed using the Metware Cloud, a free online platform for data analysis (<https://cloud.metware.cn>). The heat map is generated using TBtools 1.098 software.

Supplementary Information

The online version contains supplementary material available at <https://doi.org/10.1186/s12864-024-10054-2>.

Additional file 1.
Additional file 2.
Additional file 3.
Additional file 4.
Additional file 5.
Additional file 6.
Additional file 7.
Additional file 8.
Additional file 9.
Additional file 10.
Additional file 11.
Additional file 12.
Additional file 13.
Additional file 14.
Additional file 15.
Additional file 16.

Additional file 17.

Additional file 18.

Additional file 19.

Acknowledgements

Not applicable.

Authors' contributions

GD: Conceptualization, Data curation, Methodology, Project administration, Resources, Supervision, Writing-review & editing. LL: Formal analysis, Methodology, Validation, Writing-original draft, Writing—review & editing. Y L: Formal analysis, Validation.

Funding

This work was supported by the Science and Technology Planning Project of Guizhou Province (ZK[2022]YIBAN274; QKHPTRC[2018]5261).

Availability of data and materials

The datasets used and/or analysed during the current study are available from the corresponding author (Guijie Ding, gjding@gzu.edu.cn) on reasonable request. Transcriptome data has been deposited to National Center for Biotechnology Information (<https://www.ncbi.nlm.nih.gov/>) under BioProject ID PRJNA970846. The nucleotide sequences of *PmTPS5*, *PmTPS1*, and *PmTPPD* genes are provided in Additional File 19.

Declarations

Ethics approval and consent to participate

The plant material utilized in this study does not involve any endangered or protected species. The ongoing experimental research and field study, including the collection of plant material, adhere to relevant institutional, national, and international guidelines and legislation for the purpose of research and development. Masson pine (*Pinus massoniana*) specimens were obtained from a state-owned forest farm located in Dushan County, Guizhou Province, within the Qiannan Buyi and Miao Autonomous Prefecture. All samples were accurately identified by Jiaguo Wang. The specimens were deposited in the Tree Herbarium of the College of Forestry at Guizhou University (GZAC), with a deposition number of GZAC0031640. (<https://www.cvh.ac.cn/spms/detail.php?id=f01e49a7>).

Consent for publication

Not applicable.

Competing interests

The authors declare no competing interests.

Received: 5 September 2023 Accepted: 25 January 2024

Published online: 12 February 2024

References

- Otori K, Tanabe N, Maruyama T, Sato S, Yanagisawa S, Tamoi M, Shigeoka S. Enhanced photosynthetic capacity increases nitrogen metabolism through the coordinated regulation of carbon and nitrogen assimilation in *Arabidopsis thaliana*. *J Plant Res*. 2017;130(5):909–27.
- Cui G, Zhang Y, Zhang W, Lang D, Zhang X, Li Z, Zhang X. Response of carbon and nitrogen metabolism and secondary metabolites to drought stress and salt stress in plants. *J Plant Biol*. 2019;62(6):387–99.
- Gampe D, Zscheischler J, Reichstein M, O Sullivan M, Smith WK, Sitch S, Buermann W. Increasing impact of warm droughts on northern ecosystem productivity over recent decades. *Nat Clim Change*. 2021;11(9):772–9.
- Reich PB, Bermudez R, Montgomery RA, Rich RL, Rice KE, Hobbie SE, Stefanski A. Even modest climate change may lead to major transitions in boreal forests. *Nature*. 2022;608(7923):540–45.

5. Baslam M, Mitsui T, Sueyoshi K, Ohyama T. Recent advances in carbon and nitrogen metabolism in C3 plants. *Int J Mol Sci.* 2021;22(1):318.
6. Zhou R, Yu X, Wen J, Jensen NB, Dos Santos TM, Wu Z, Rosenqvist E, Ottosen C. Interactive effects of elevated CO₂ concentration and combined heat and drought stress on tomato photosynthesis. *BMC Plant Biol.* 2020;20(1):260.
7. Kruse J, Adams M, Winkler B, Ghirardo A, Alfarraj S, Kreuzwieser J, Hedrich R, Schnitzler JP, Rennenberg H. Optimization of photosynthesis and stomatal conductance in the date palm *Phoenix dactylifera* during acclimation to heat and drought. *New Phytol.* 2019;223(4):1973–88.
8. Collins AD, Ryan MG, Adams HD, Dickman LT, Garcia Forner N, Grosziord C, Powers HH, Sevanto S, McDowell NG. Foliar respiration is related to photosynthetic, growth and carbohydrate response to experimental drought and elevated temperature. *Plant Cell Environ.* 2021;44(12):3853–65.
9. Coast O, Posch BC, Bramley H, Gaju O, Richards RA, Lu M, Ruan Y, Trethowan R, Atkin OK. Acclimation of leaf photosynthesis and respiration to warming in field-grown wheat. *Plant Cell Environ.* 2020;44(7):2331.
10. Zandalinas SI, Mittler R, Balfagón D, Arbona V, Gómez Cadenas A. Plant adaptations to the combination of drought and high temperatures. *Physiol Plant.* 2018;162(1):2–12.
11. Quan W, Ding G. Root tip structure and volatile organic compound responses to drought stress in masson pine (*Pinus massoniana* Lamb). *Acta Physiol Plant.* 2017;39(12):1.
12. Deng X, Xiao W, Shi Z, Zeng L, Lei L. Combined effects of Drought and Shading on Growth and non-structural carbohydrates in *Pinus massoniana* Lamb. Seedlings. *Forests.* 2020;11(1):18.
13. Correia P, Da SA, Vaz M, Carmo-Silva E, Marques DSJ. Efficient regulation of CO₂ assimilation enables greater resilience to high temperature and drought in maize. *Front Plant Sci.* 2021;12:675546.
14. Xue G, McIntyre CL, Jenkins CLD, Glassop D, van Herwaarden AF, Shorter R. Molecular dissection of variation in carbohydrate metabolism related to water-soluble carbohydrate accumulation in stems of wheat. *Plant Physiol.* 2008;146(2):323–4.
15. Xu B, Hu W, Gao M, Zhao W, Wang Y, Zhou Z. Effects of elevated air temperature coupling with soil drought on carbohydrate metabolism and oil synthesis during cottonseed development. *Physiol Plant.* 2022;174(1):e13643.
16. Wenting W, Wenpei C, Ke X, Hui G, Haiyan W, Hongcheng Z. Effects of early- and late-sowing on starch accumulation and associated enzyme activities during grain filling stage in rice. *Rice Sci.* 2021;28(2):191–9.
17. Liu MS, Chien CT, Lin TP. Constitutive components and induced gene expression are involved in the desiccation tolerance of selaginella tamari-scina. *Plant Cell Physiol.* 2008;49(4):653–63.
18. Drennan PM, Smith MT, Goldsworthy D, van Staden J. The occurrence of trehalose in the leaves of the desiccation-tolerant angiosperm *myrothamnus flabellifolius* Welw. *J Plant Physiol.* 1993;142(4):493.
19. Li LL, Li Y, Ding GJ. Research progress on effects of high temperature and drought on carbon metabolism in woody plants. *J Mountain Agric Biol.* 2022;41(6):30–6.
20. Duan H, Wu J, Huang G, Zhou S, Liu W, Liao Y, Yang X, Xiao Z, Fan H. Individual and interactive effects of drought and heat on leaf physiology of seedlings in an economically important crop. *AOB Plants.* 2016;9(1):plw090.
21. Khatun M, Sarkar S, Era FM, Islam AKMM, Anwar MP, Fahad S, Datta R, Islam AKMA. Drought stress in grain legumes: effects, tolerance mechanisms and management. *Agronomy.* 2021;11(12): 2374.
22. Flexas J, Barón M, Bota J, Ducruet J, Gallé A, Galmés J, Jiménez M, Pou A, Ribas-Carbo M, Sajani C, et al. Photosynthesis limitations during water stress acclimation and recovery in the drought-adapted *Vitis hybrid* richter-110 (*V. berlandieri* × *V. rupestris*). *J Exp Bot.* 2009;60(8):2361–77.
23. Aparecido LMT, Woo S, Suazo C, Hultine KR, Blonder B. High water use in desert plants exposed to extreme heat. *Ecol Lett.* 2020;23(8):1189–200.
24. Marchin RM, Backes D, Ossola A, Leishman MR, Tjoelker MG, Ellsworth DS. Extreme heat increases stomatal conductance and drought-induced mortality risk in vulnerable plant species. *Glob Change Biol.* 2022;28(3):1133–46.
25. Yan W, Zhong Y, Shangguan Z. A meta-analysis of leaf gas exchange and water status responses to drought. *Sci Rep-UK.* 2016;6(1):20917.
26. Singh J, Pandey P, James D, Chandrasekhar K, Achary VM, Kaul T, Tripathy BC, Reddy MK. Enhancing C3 photosynthesis: an outlook on feasible interventions for crop improvement. *Plant Biotechnol J.* 2014;12(9):1217–30.
27. Zhou Y, Lam HM, Zhang J. Inhibition of photosynthesis and energy dissipation induced by water and high light stresses in rice. *J Exp Bot.* 2007;58(5):1207–17.
28. Pelloux J, Jolivet Y, Fontaine V, Banvoy J, Dizengremel P. Changes in Rubisco and Rubisco activase gene expression and polypeptide content in *Pinus halepensis* M. subjected to ozone and drought. *Plant Cell Environ.* 2001;24(1):123.
29. Sukanami M, Suzuki Y, Tazoe Y, Yamori W, Makino A. Co-overproducing Rubisco and Rubisco activase enhances photosynthesis in the optimal temperature range in rice. *Plant Physiol.* 2020; 185(1):108–19.
30. Salvucci ME, Crafts-Brandner SJ. Relationship between the heat tolerance of photosynthesis and the thermal stability of Rubisco activase in plants from contrasting thermal environments. *Plant Physiol.* 2004;134(4):1460–70.
31. Galmes J, Aranjuelo I, Medrano H, Flexas J. Variation in Rubisco content and activity under variable climatic factors. *Photosynth Res.* 2013;117(1–3):73–90.
32. Ruan Y. Signaling role of sucrose metabolism in development. *Mol Plant.* 2012;5(4):763–5.
33. Oktyabrsky ON, Smirnova GV. Redox regulation of cellular functions. *Biochem Biokhimiia.* 2007;72(2):132.
34. Christine HF, Graham N. Oxidant and antioxidant signalling in plants: a re-evaluation of the concept of oxidative stress in a physiological context. *Plant Cell Environ.* 2005;28(8):1056.
35. Bolouri-Moghaddam MR, Le Roy K, Xiang L, Rolland F, Van den Ende W. Sugar signalling and antioxidant network connections in plant cells. *FEBS J.* 2010;277(9):2022–37.
36. Liu J, Wang X, Hu Y, Hu W, Bi Y. Glucose-6-phosphate dehydrogenase plays a pivotal role in tolerance to drought stress in soybean roots. *Plant Cell Rep.* 2013;32(3):415–29.
37. Sunkar R, Kapoor A, Zhu J. Posttranscriptional Induction of Two Cu/Zn Superoxide dismutase genes is mediated by downregulation of miR398 and important for oxidative stress tolerance. *Plant Cell.* 2006;18(8):2051–65.
38. Sinkevich MS, Naraykina NV, Trunova TI. Involvement of sugars in the antioxidant defense against paraquat-induced oxidative stress in potato transformed with yeast invertase gene. *Dokl Biol Sci.* 2010;434:338–40.
39. Van den Ende W, Valluru R. Sucrose, sucrosyl oligosaccharides, and oxidative stress: scavenging and salvaging? *J Exp Bot.* 2008;60(1):9–18.
40. Mittler R, Blumwald E. Genetic engineering for modern agriculture: challenges and perspectives. *Annu Rev Plant Biol.* 2010;61:443–62.
41. Alizadeh Yeloojeh K, Saeidi G, Sabzaljan MR. Drought stress improves the composition of secondary metabolites in safflower flower at the expense of reduction in seed yield and oil content. *Ind Crop Prod.* 2020;154: 112496.
42. Schiraldi C, Di Lernia I, De Rosa M. Trehalose production: exploiting novel approaches. *Trends Biotechnol.* 2002;20(10):420–5.
43. Iturriaga G, Cushman MAF, Cushman JC. An EST catalogue from the resurrection plant *Selaginella lepidophylla* reveals abiotic stress-adaptive genes. *Plant Sci.* 2006;170(6):1173–84.
44. Ambastha V, Tiwari BS. Cellular water and anhydrobiosis in plants. *J Plant Growth Regul.* 2015;34(3):665–71.
45. Kaplan F, Kopka J, Haskell DW, Zhao W, Schiller KC, Gatzke N, Sung DY, Guy CL. Exploring the temperature-stress metabolome of *Arabidopsis*. *Plant Physiol.* 2004;136(4):4159–68.
46. Han B, Fu L, Zhang D, He X, Chen Q, Peng M, Zhang J. Interspecies and Intraspecies Analysis of trehalose contents and the biosynthesis pathway gene family reveals crucial roles of trehalose in osmotic-stress tolerance in cassava. *Int J Mol Sci.* 2016;17(7): 1077.
47. Luo Y, Gao YM, Wang W, Zou CJ. Application of trehalose ameliorates heat stress and promotes recovery of winter wheat seedlings. *BIOL Plant.* 2014;58(2):395–8.
48. Luo Y, Xie Y, He D, Wang W, Yuan S. Exogenous trehalose protects photosystem II by promoting cyclic electron flow under heat and drought stresses in winter wheat. *Plant Biol (Stuttg).* 2021;23(5):770–6.
49. Li H, Zang B, Deng X, Wang X. Overexpression of the trehalose-6-phosphate synthase gene *OstPS1* enhances abiotic stress tolerance in rice. *Planta.* 2011;234(5):1007–18.

50. Jiang D, Chen W, Gao J, Yang F, Zhuang C. Overexpression of the trehalose-6-phosphate phosphatase OsTPP3 increases drought tolerance in rice. *Plant Biotechnol Rep.* 2019;13(3):285–92.
51. Lin Q, Yang J, Wang Q, Zhu H, Chen Z, Dao Y, Wang K. Overexpression of the trehalose-6-phosphate phosphatase family gene AtTPPF improves the drought tolerance of *Arabidopsis thaliana*. *BMC Plant Biol.* 2019;19(1):381.
52. Lin Q, Gong J, Zhang Z, Meng Z, Wang J, Wang S, Sun J, Gu X, Jin Y, Wu T, et al. The *Arabidopsis thaliana* trehalose-6-phosphate phosphatase gene AtTPPI regulates primary root growth and lateral root elongation. *Front Plant Sci.* 2023;13:1088278.
53. Nuccio ML, Wu J, Mowers R, Zhou H, Meghji M, Primavesi LF, Paul MJ, Chen X, Gao Y, Haque E, et al. Expression of trehalose-6-phosphate phosphatase in maize ears improves yield in well-watered and drought conditions. *Nat Biotechnol.* 2015;33(8):862–9.
54. Trapnell C, Hendrickson DG, Sauvageau M, Goff L, Rinn JL, Pachter L. Differential analysis of gene regulation at transcript resolution with RNA-seq. *Nat Biotechnol.* 2013;31(1):46–53.
55. Wan L, Li B, Lei Y, Yan L, Ren X, Chen Y, Dai X, Jiang H, Zhang J, Guo W, et al. Mutant transcriptome sequencing provides insights into pod development in peanut (*Arachis hypogaea* L.). *Front Plant Sci.* 2017;8:8.

Publisher's Note

Springer Nature remains neutral with regard to jurisdictional claims in published maps and institutional affiliations.